Strength and Stiffness Analyses of Standard and Double Mortise and Tenon Joints

Seid Hajdarevic,[a,*] Murco Obucina,[a] Elmedin Mesic,[b] and Sandra Martinovic [a]

This paper investigated the effect of the tenon length on the strength and stiffness of the standard mortise and tenon joints, as well of the double mortise and tenon joints, that were bonded by poly(vinyl acetate) (PVAc) and polyurethane (PU) glues. The strength was analyzed by measuring applied load and by calculating ultimate bending moment and bending moment at the proportional limit. Stiffness was evaluated by measuring displacement and by calculating the ratio of applied force and displacement along the force line. The results were compared with the data obtained by the simplified static expressions and numerical calculation of the orthotropic linear-elastic model. The results indicated that increasing tenon length increased the maximal moment and proportional moment of the both investigated joints types. The analytically calculated moments were increased more than the experimental values for both joint types, and they had generally lower values than the proportional moments for the standard tenon joints, as opposed to the double tenon joints. The Von Mises stress distribution showed characteristic zones of the maximum and increased stress values. These likewise were monitored in analytical calculations. The procedures could be successfully used to achieve approximate data of properties of loaded joints.

Keywords: Mortise and tenon joint; Strength; Stiffness; Tenon length; Glue; Finite element method

Contact information: a: Department of Wood Technology, Faculty of Mechanical Engineering, University of Sarajevo, 71000, Sarajevo, Bosnia and Herzegovina; b: Department of Mechanical Design, Faculty of Mechanical Engineering, University of Sarajevo, 71000, Sarajevo, Bosnia and Herzegovina;
** Corresponding author: hajdarevic@mef.unsa.ba*

INTRODUCTION

Mortise and tenon joints have a wide range of use in furniture frame construction. Although this type of joint is a common and basic way of connecting wooden elements into a frame, there is still a considerable interest in analyzing the existing and developing new forms of the tenon joint. A better understanding of specific mechanical properties of tenon joints can lead to improvement of quality of furniture frame structure.

There are numerous factors that affect the mechanical properties of loaded profile-adhesive joints. The bending moment capacity of the window joints shows a statistically significant difference between bending moments for the tenon and dowel joints, and the absence of difference between the compression and tension for both joint types (Podlena *et al.* 2017). The factors that affect the moment capacity, and the main effects and interaction factors affecting the moment capacity for both compression and tension loads of the mortise and tenon joints have been investigated (Kasal *et al.* 2015). Tenon size (width and length) affects the bending moment capacity, and joint capacity is most affected by tenon length. In addition, shear strength of the wood parallel to grain has a substantial

effect, while the adhesives have a measurable effect on the joint capacity.

The mortise and tenon furniture joins became stronger and stiffer as either tenon width or length increased. Tenon length has a greater effect on moment resistance, while tenon width has more effect on stiffness (Wilczyński and Warmbier 2003; Kasal *et al.* 2016). Mortise and tenon joints with tight-fitting shoulders have greater bending moment capacity than those with loose fitting shoulders; in addition, tenon shoulders substantially decrease rotation factors. Tenon cross-section also has a substantial effect on bending moment capacity. Joints with a round tenon configuration have only half of the capacity values of those with rectangular tenon configuration (Likos *et al.* 2012). The bending moment capacity is directly related to the depth of embedment of the tenons and strongly related to shoulder width, whereas tenon width have a lesser effect (Derikvand *et al.* 2014). Analysis of stiffness coefficients of mortise and tenon joints used on wooden window profiles confirmed that type of load did not affect the stiffness of the joint, but the width of joint did affect the stiffness (Podlena and Boruvka 2016). The effect of fitting for pairing of open full-width mortise and tenon joint elements on the compressive strength of the joint has been investigated. The mortise and tenon joints were found to be the strongest at a tight fit of 0.1 mm (Elek *et al.* 2020).

The results of investigation of the strength of the two most frequent joints in the upholstered furniture frames (mortise and tenon joints and double dowel joints), constructed with two wood species and the use of two adhesives (PVAc and PU) showed that the mortise and tenon joint in combination with PVAc, provided the best strength for all investigated wood species (Vassiliou *et al.* 2016). In an investigation of effect of wood species and adhesive type on the stiffness of rail to leg mortise and tenon furniture joints, the type of glue was not important for spruce joints, whereas for beech, the stiffness of joints glued with PVAc was significantly higher than with PU adhesive (Záborský *et al.* 2017). In comparison with PVAc, PU glue has appropriate strength, and, as they slightly expand during the hardening phase, can completely fill and cover the gaps between elements of joint (Hrovatin *et al.* 2013). Dowel joints glued with PU adhesive showed improved mechanical properties in humid environments (Máchová *et al.* 2019). The improved bonding properties of PVAc glue and bending and tension strength of the mortise and tenon joints has been achieved by using nano-fillers and its good dispersion provided at the low loadings of nano-fillers to PVAc matrix (Bardak *et al.* 2017).

Numerical methods, such as the 'finite element method', are applicable and effective for the analysis of orthotropic structures. The numerical results depend on simplifications and assumptions introduced in the numerical model. Numerical analyses give reasonable estimates of mechanical properties of wood constructions and their joints (Smardzewski 2008; Horman *et al.* 2010; Hajdarević and Martinović 2014; Hajdarević and Busuladžić 2015; Hu and Guan 2017; Hu *et al* 2019a, b).

This study investigated the effect of the tenon length on the mechanical properties of mortise tenon joints taken from a manufacturing process with two different joint geometry that were bonded by three glue types. In addition, the objective was to explore the capabilities of analytical and numerical calculation in design optimization of a frame joint. The strength and stiffness of the standard and double mortise and tenon joints were determined, and the results were compared by the simplified static expressions and numerical calculations of the linear-elastic model.

EXPERIMENTAL

Materials and Specimens

The thirty-six (36) corners mortise and tenon joints that were supplied from furniture manufacturers (MS&WOOD, Fojnica, Bosnia and Herzegovina) were analyzed (Fig. 1). All joints were made from beech wood (*Fagus sylvatica* L.), with round peg shape and mortise and tenon interference fit. The first set of joints contained 18 standard mortise and tenon joints with cross section of elements of 50 × 30 mm (Fig. 1a), while the second set of joints contained 18 double mortise and tenon joints with cross section of elements 50 × 40 mm and overhanging end (Fig. 1b). The joints were constructed by using two different tenon lengths (20 and 30 mm), with 9 replications of each two joint sets. Two types of glue (PVAc and PU) were utilized for assembling the joint specimens. The three joints specimens, within each joint set and tenon length, were bonded with PVAc glue manufactured by AkzoNobel (PVAc1; Akzo Nobel N.V., Amsterdam, Netherlands) and by Kleiberit 303 D3 (PVAc2; Klebchemie, Weingarten, Germany). Three specimens were bonded with Jowat Power – PUR 687.40 glue (PU; Jowat SE, Detmold, Germany). The moisture content (MC) was evaluated in accordance with procedures describe in ISO 13061-1 (2014) after testing. The average MC value was 12.1%.

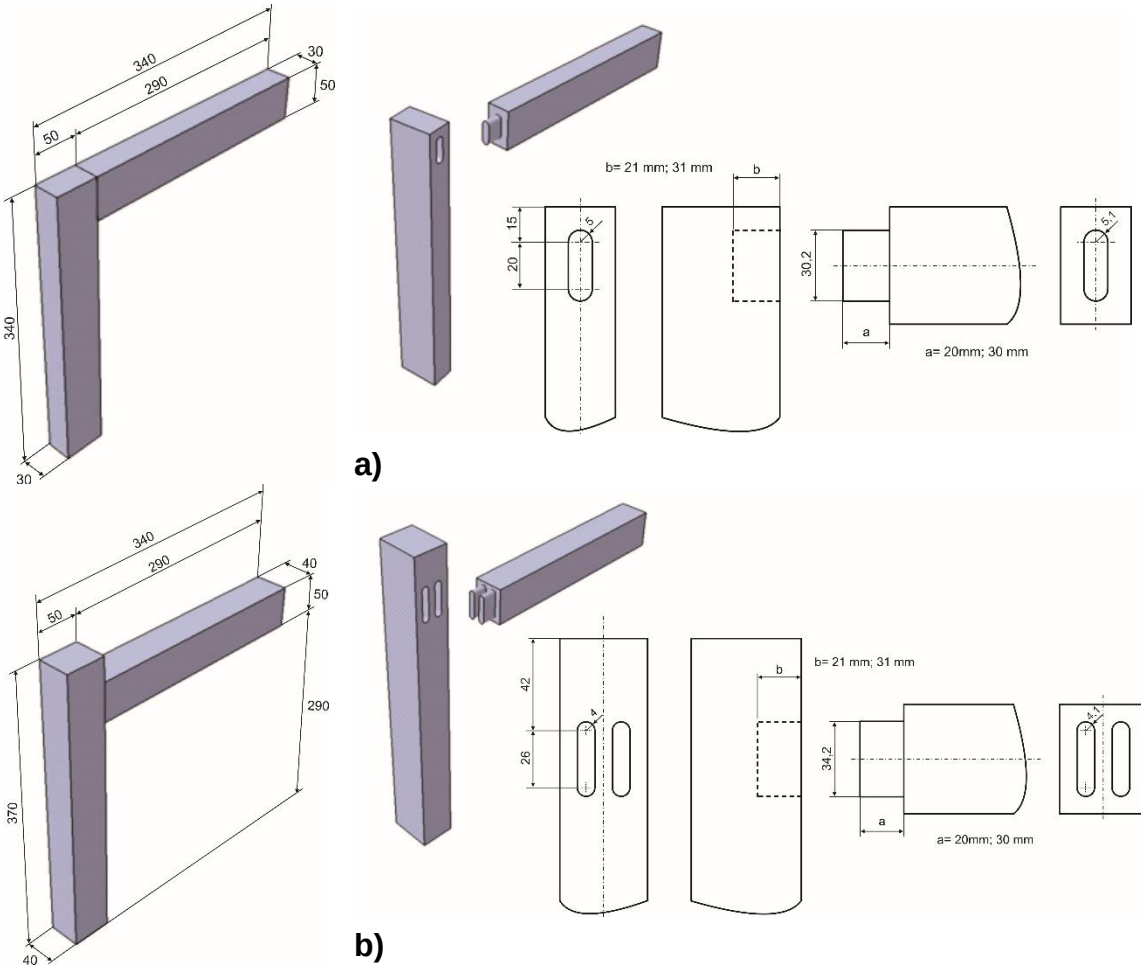

Fig. 1. Test samples geometry: a) configuration of the standard mortise and tenon joints with two size of tenon lengths, b) configuration of the double mortise and tenon joints with overhanging end and two size of tenon lengths

Method of Testing

The loading diagram of the joints is shown in Fig. 2a. The joint was pin connected on the lower edge. The roller support was set up on the upper joint edge. The load was applied to the joint in a manner that corresponded to compression of specimen. The test was carried out on a universal testing machine Zwick 1435 (Zwick Roell Group, Ulm, Germany), and the rate of static loading was 10 mm/min, Fig. 2b. The load value was continuously recorded by load cell RSCC-C3/1t (HBM, Darmstadt, Germany). The displacement of the defined point in the direction of the force *F* during the testing was measured by inductive displacement transducer WI10 (HBM, Darmstadt, Germany). The force and the displacement along the force line were measured simultaneously until a large drop in the load occurred by data acquisition (DAQ) system QuantumX MX840B (HBM, Darmstadt, Germany). Display and processing of measurement results were performed using the DAQ software Catman (HBM, Darmstadt, Germany) The working diagrams of the tested specimens were created. Figure 2c shows the curve of force-displacement diagram with elastic region defined on the basis proportional forces $0.4 \cdot F_{max}$ and $0.6 \cdot F_{max}$ as well as the proportional limit point. Increased displacements that occurred at the beginning of loading were neglected in data analysis.

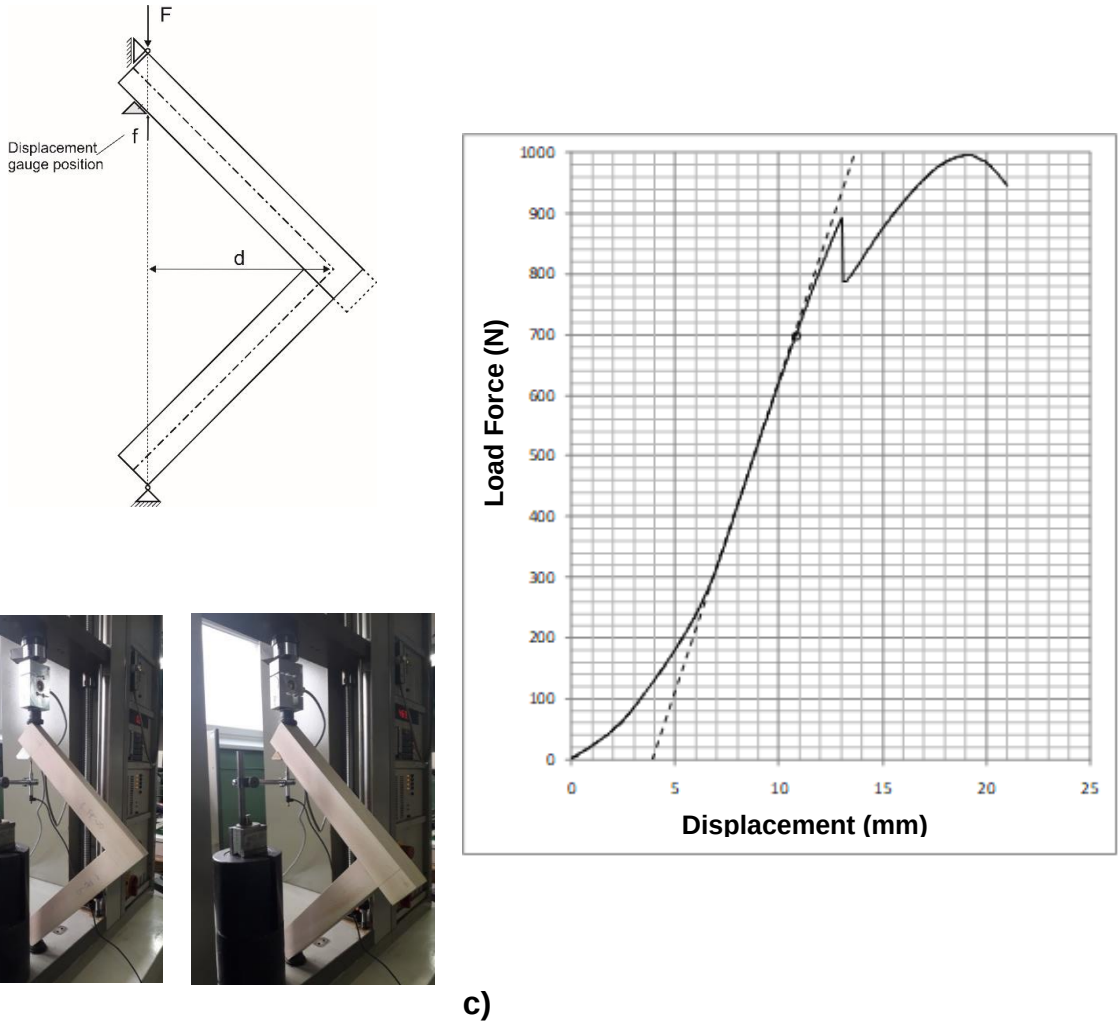

Fig. 2. Joints testing: a) the diagram of joint loading, b) set-up of standard and double mortise and tenon joints in the testing machine, c) working diagram of joint strength testing

The ultimate applied load values (F_{max}) and the load at the proportional limit (F_p) were ascertained using the software collected data. Corresponding bending moment values of the joints were calculated in Nm by expressions $M_{max}=F_{max}\cdot d$ and $M_p=F_p\cdot d$ for ultimate bending moment and bending moment at the proportional limit, respectively. The moment arm, the perpendicular distance from the force line to the point of intersection of symmetry axis of the elements, was d = 205.06 mm for both set of joints, as shown in Fig. 2a. The values of displacements at the ultimate applied load (δ_{max}) and displacements at the proportional limit (δ_p) were ascertained using the software collected data and were used for calculation of stiffness that was defined by ratios F_{max}/δ_{max} and F_p/δ_p for ultimate load and load at the proportional limit, respectively. The ratios were calculated in N/mm.

Analytical Calculation of Joints Strength

The strength of mortise and tenon joints was calculated by means of the common simplified static expressions to determine reaction moment of a loaded joint. Figure 3 presents a generalized scheme of analytical consideration of stress distribution on the characteristic support surface of tenon and tenon shoulder along with the required dimensions. The total reaction moment of a joint (1) is the sum of the simultaneous reaction moments obtained on the basis of defined stresses that occur on the characteristic support surfaces of the profile-adhesive joint, Fig. 3a,

$$M_R = M_1 + M_2 + M_3 \quad (1)$$

where M_R is total reaction moment, M_1 is moment of the edge cheek, M_2 is moment of the structural shoulder and M_3 is moment of the face cheek.

Reaction moments were calculated using the joint dimensions, the number of glue lines and relevant stress (permissible stress or strength of used material), Fig. 3b.

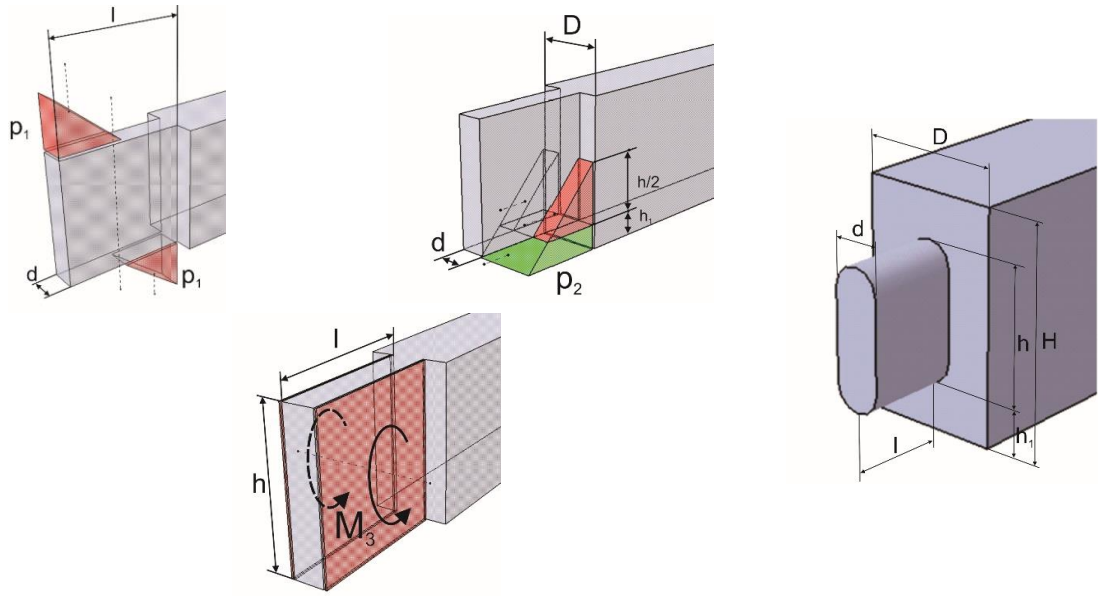

Fig. 3. Reaction moments of a loaded joint: a) generalized scheme of stress distribution on the characteristic support surfaces, b) relevant dimensions of standard and double mortise and tenon joints

The moment of the edge cheek M_1 and the reaction moment of structural shoulder M_2 were obtained by the following equations,

$$M_1 = \sigma_1 \frac{l^2 d}{6} \quad (2)$$

$$M_2 = \frac{\sigma_2}{3}\left[\left(\frac{h}{2} + h_1\right)^2 D - \frac{\left(\frac{h}{2}\right)^3}{\left(\frac{h}{2}+h_1\right)} d\right] \quad (3)$$

where σ_1 and σ_2 are negative normal stress *i.e.* compression strength of wood normal to the fibers (Pa), and other notations are shown in Fig. 3b. Moment in the plane of face cheek M_3 was obtained by Eq. 3,

$$M_3 = n\,\beta\,h\,l^2\,\tau \quad (4)$$

where n is the number of face cheeks, τ is shear stress *i.e.* strength of glue line (Pa), β is the Saint-Venant coefficient shown in Eq. 5,

$$\frac{1}{\beta} = 3 + \frac{2{,}6}{0{,}45+\frac{h}{l}} \quad (5)$$

where dimensions h and l are tenon width and tenon length.

Numerical Analysis of Joints

The total reactive moments of joints obtained from analytical calculation were used in a simplified numerical analysis of stress and strain of the loaded joints. The physical model is defined based on the experimental loading diagram of the joints and local coordinates are used to define the grain directions of the joint elements, as shown in Fig. 4. Loading forces (F_l) of each model of joints were calculated by the equation $F_l = M_R / d$ where M_R is analytical total reaction moment and d is the moment arm.

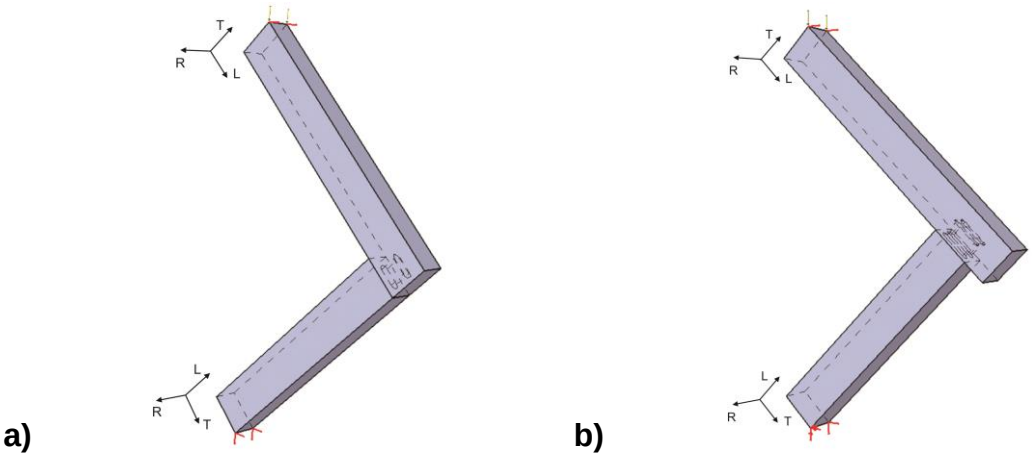

Fig. 4. The physical model of the joints: a) standard mortise and tenon joint (tenon length 20 mm), b) double mortise and tenon joint (tenon length 20 mm)

Numerical 3D linear-elastic model for orthotropic material was solved by a method based on the finite elements. Mesh model of standard mortise and tenon joint, along with mesh details of standard and double tenon joints are shown in Fig. 5. The 10-node parabolic tetrahedron finite element was used to create numerical model. The mesh was selectively refined to obtain a better results accuracy. A fastened connection was modeled between

surfaces of mortise and tenon while among other surfaces *i.e.* tenon shoulder and mortise side wall a contact connection was used. Calculation was carried out for beech wood and the elastic properties of the wood are presented in Table 1 (Smardzewski 2008). Adhesive, *i.e.*, glue line and interference fit were neglected. The numerical results were obtained using the CAD/CAM/CAE system CATIA (Dassault Systemes SE, Velizy-Villacoublay, France).

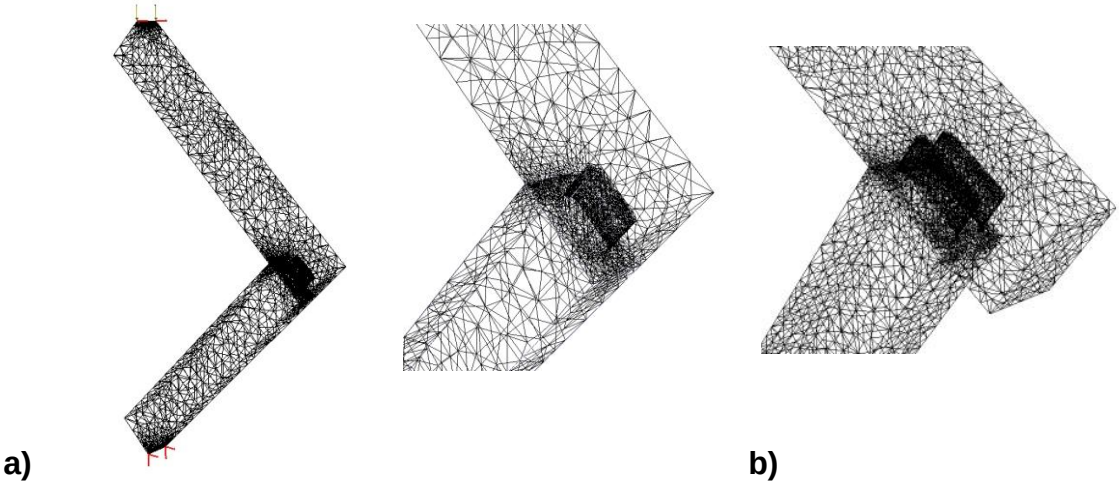

Fig. 5. Numerical models of the joints: a) mesh of standard mortise and tenon joint with boundary conditions (tenon length 20 mm), b) details of standard and double mortise and tenon joints mesh (tenon length 20 mm)

Table 1. Elastic Properties of Beech Wood (Smardzewski 2008)

Modulus of Elasticity (GPa)			Modulus of Rigidity (GPa)			Poisson's Ratio					
E_L	E_R	E_T	G_{LR}	G_{LT}	G_{RT}	ν_{LR}	ν_{LT}	ν_{RT}	ν_{TR}	ν_{RL}	ν_{TL}
13.969	2.284	1.160	1.645	1.082	0.471	0.450	0.510	0.750	0.360	0.075	0.044

RESULTS AND DISCUSSION

The experimental results of maximal (F_{max}) and proportional force (F_p), maximal moment (M_{max}) and proportional moment (M_p) and ratio of proportional and maximal moment (M_p /M_{max}) of the standard tenon joints and double tenon joints with two different tenon lengths are given in Tables 2 and 3, respectively.

Generally, the results indicated that average bending moment (both maximum moment and proportional moment) of standard tenon joints and double tenon joints and for all investigated types of glue increased as the tenon length increased. Also, the results show relatively large differences among the average bending moment and the average proportional moments of mortise and tenon joints bonded by PVAc1, PVAc2, and PU. The differences are the results of a high slope of the proportional lines that have been fitted to the curves of force-displacement relationship in order to neglect the initial large displacements that occurred at the beginning of loading.

Table 2. Experimental Results of Forces and Bending Moments of the Standard Mortise and Tenon Joints

Standard mortise and tenon joint													
Tenon length 20 mm							Tenon length 30 mm						
Glue	Joint No.	F_{max} (N)	F_p (N)	M_{max} (Nm)	M_p (Nm)	M_p / M_{max}	Glue	Joint No.	F_{max} (N)	F_p (N)	M_{max} (Nm)	M_p (Nm)	M_p / M_{max}
PVAc1	1	995.45	697.96	204.13	143.12	0.70	PVAc1	1	1405.77	952.42	288.27	195.30	0.68
	2	1311.22	873.19	268.88	179.06	0.67		2	1439.13	831.90	295.11	170.59	0.58
	3	1091.08	824.77	223.74	169.13	0.76		3	1398.14	936.65	286.70	192.07	0.67
	Ave.	1132.58	798.64	232.25	163.77	0.71		Ave.	1414.35	906.99	290.03	185.99	0.64
PVAc2	1	865.23	730.86	177.42	149.87	0.84	PVAc2	1	1198.14	796.42	245.69	163.31	0.66
	2	1023.00	708.50	209.78	145.29	0.69		2	-	-	-	-	-
	3	1058.32	835.19	217.02	171.26	0.79		3	1186.53	754.98	243.31	154.82	0.64
	Ave.	982.18	758.18	201.41	155.47	0.77		Ave.	1192.34	775.70	244.50	159.07	0.65
PU	1	1271.22	872.90	260.68	179.00	0.69	PU	1	1471.94	956.35	301.84	196.11	0.65
	2	1001.60	704.96	205.39	144.56	0.70		2	1563.66	956.03	320.64	196.04	0.61
	3	1010.29	716.30	207.17	146.88	0.71		3	1552.99	1081.09	318.46	221.69	0.70
	Ave.	1094.37	764.72	224.41	156.81	0.70		Ave.	1529.53	997.82	313.65	204.61	0.65

Table 3. Experimental Results of Forces and Bending Moments of the Double Mortise and Tenon Joints

Double mortise and tenon joint													
Tenon length 20 mm							Tenon length 30 mm						
Glue	Joint No.	F_{max} (N)	F_p (N)	M_{max} (Nm)	M_p (Nm)	M_p / M_{max}	Glue	Joint No.	F_{max} (N)	F_p (N)	M_{max} (Nm)	M_p (Nm)	M_p / M_{max}
PVAc1	1	1708.84	1049.56	350.42	215.22	0.61	PVAc1	1	1638.84	1073.75	336.06	220.18	0.66
	2	1485.43	913.02	304.60	187.22	0.61		2	1842.31	1189.43	377.78	243.91	0.65
	3	1830.14	1162.95	375.29	238.47	0.64		3	2479.71	1453.86	508.49	298.13	0.59
	Ave.	1674.80	1041.84	343.43	213.64	0.62		Ave.	1986.95	1239.01	407.44	254.07	0.62
PVAc2	1	1902.34	1286.61	390.09	263.83	0.68	PVAc2	1	2098.28	1315.27	430.27	269.71	0.63
	2	1766.90	1099.59	362.32	225.48	0.62		2	2022.27	1279.31	414.69	262.33	0.63
	3	1879.69	1156.01	385.45	237.05	0.61		3	1660.90	1235.61	340.58	253.37	0.74
	Ave.	1849.64	1180.74	379.29	242.12	0.64		Ave.	1927.15	1276.73	395.18	261.81	0.66
PU	1	1621.02	1105.05	332.41	226.60	0.68	PU	1	2268.87	1649.37	465.25	338.22	0.73
	2	1142.50	692.42	234.28	141.99	0.61		2	1806.83	1229.71	370.51	252.16	0.68
	3	1572.69	973.29	322.50	199.58	0.62		3	2202.59	1308.32	451.66	268.28	0.59
	Ave.	1445.40	923,59	296.39	189.39	0.64		Ave.	2092.76	1395.80	429.14	286.22	0.67

The standard mortise and tenon joints glued with PVAc2 had the lowest average bending moment (201.4 Nm, 244.5 Nm) and average proportional moments (155.5 Nm, 159.1 Nm) for tenon length 20 mm and 30 mm, respectively. The joints glued with PVAc1 for tenon length 20 mm and the joints glued with PU for tenon length 30 mm had the highest average bending moment and proportional moment. The maximal bending moment (average value) increased by 24.9% (PVAc1), 21.4% (PVAc2) and 39.8% (PU) as tenon length increased from 20 mm to 30 mm for standard mortise and tenon joint. The joints with tenon length 30 mm had 13.6% (PVAc1), 2.3% (PVAc2) and 30.9% (PU) higher proportional bending moments (average value) than the joints with tenon length 20 mm. Normalized ratios of average values of proportional and maximal moment of the standard tenon joints with tenon length 20 mm were 71% (PVAc1), 77% (PVAc2) and 70% (PU). These percentages were lower for the standard tenon joints with tenon length 30 mm and those percentages are 64% (PVAc1), 65% (PVAc2) and 65% (PU).

The double mortise and tenon joints glued with PU had the lowest average bending moment (296.4 Nm) and average proportional moment (189.4 Nm) for tenon length 20 mm and also had the highest average bending moment (429.1 Nm) and average proportional moment (286.2 Nm) for tenon length 30 mm. The maximal bending moment of double mortise and tenon joints with tenon length 30 mm were 18.6% (PVAc1), 4.2% (PVAc2) and 44.8% (PU) higher than the average value for the double tenon joints with tenon length 20 mm. The average proportional moment increased by 18.9% (PVAc1), 8.1% (PVAc2) and 51.1% (PU) as tenon length increased from 20 mm to 30 mm for double mortise and tenon joint. The percentages of the average ratio of proportional and maximal moments of the double tenon joints with tenon length 20 mm were 62% (PVAc1), 64% (PVAc2) and 64% (PU), while they were 62% (PVAc1), 66% (PVAc2) and 67% (PU) for the double tenon joints with tenon length 30 mm.

The differences between the average value of maximum moment (bending moment capacities) of standard tenon joints and double tenon joints were clearly observed. However, these values were not comparable due to the dimensional differences of these two types of joints (thickness and width of tenon and thickness of joint elements). The presented experimental results are unable to determine the dimensional effect on the joints maximum bending moment. Also, the characteristic patterns of fractures of certain types of joints were not observed. Wood fracture of the joint member, tenon fracture or tenon pulled out from the member, as glue line failed and the tenon started to take the load, occurred in all sets of standard and double joints, as shown in Fig. 6.

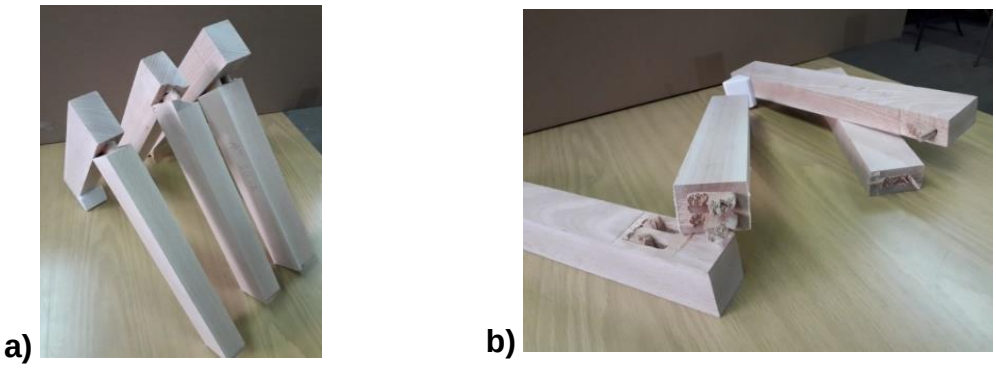

Fig. 6. Type of standard and double joints failures: a) tenons pull out from the members after the glue line fractured and the fracture of wood of a joint member, b) the fracture of joints tenons

The analytical calculation results of the reaction moments, total reaction moment M_R, and ratio of total reaction moment for tenon lengths 20 mm and tenon lengths 30 mm of the standard and double tenon joints are given in Table 4. The compression strength of beech wood normal to the fibers (negative normal stresses σ_1 and σ_2) and the generalized strength of a glue line (shear stress) that was used in the calculation was 10 MPa (Skarvelis and Mantanis 2013; Derikvand and Pangh 2016).

Table 4. Analytical Calculation of Reaction Moments of Standard and Double Tenon Joints

Reaction moments (Nm)	Standard mortise and tenon joint		Double mortise and tenon joint	
	Tenon length		Tenon length	
	20 mm	30 mm	20 mm	30 mm
M_1	6.80	15.30	5.47	12.30
M_2	57.82	57.82	72.40	72.40
M_3	55.84	113.61	130.20	265.62
M_R	120.46	186.73	208.07	350.32
$M_{R\,20}$ / $M_{R\,30}$	0.65		0.59	

Table 5. Ratio of Calculated Reaction Moments and Experimental Moments of Standard and Double Tenon Joints

Glue	Standard mortise and tenon joint				Glue	Double mortise and tenon joint			
	Tenon length					Tenon length			
	20 mm		30 mm			20 mm		30 mm	
	M_R/M_{max}	M_R/M_P	M_R/M_{max}	M_R/M_P		M_R/M_{max}	M_R/M_P	M_R/M_{max}	M_R/M_P
PVAc1	0.52	0.74	0.64	1.00	PVAc1	0.61	0.97	0.86	1.38
PVAc2	0.60	0.77	0.76	1.17	PVAc2	0.55	0.86	0.89	1.34
PU	0.54	0.77	0.60	0.91	PU	0.70	1.1	0.82	1.22

The moment of the edge cheek M_1 and the reactive moment in the plane of the face cheek M_3 for tenon length 20 mm were 55.5% and 50.9% lower than the value for joints with tenon length 30 mm for both standard and double joints, respectively. Apparently, the value of the reaction moment of structural shoulder M_2 did not change. The percentages of

the ratio of total reaction moment for tenon lengths 20 mm and tenon lengths 30 mm were 65% and 59% for the standard tenon joints and for the double tenon joints, respectively.

The ratio of calculated total reaction moments and experimental moments for the standard and double tenon joints and tenon lengths 20 and 30 mm are given in Table 5. The results indicated that the reactive moment obtained by the analytical calculation does not represent the value of the bending moment capacities of joint. The reactive moment can be taken as the estimated value of the proportional moment of the loaded joint.

The total reaction moments were no higher than bending moment capacities. The percentages of the ratio of total reaction moments and average maximum moments (bending moment capacities) for tenon lengths 20 mm were ranged from 52% to 60% for the standard tenon joints and from 55% to 70% for the double tenon joints. The percentages of the same ratio for tenon lengths 30 mm were higher and ranged from 60% to 76% for the standard tenon joints and from 82% to 89% for the double tenon joints.

In general, the total reaction moments were lower than proportional moments for tenon length 20 mm or higher than proportional moments for tenon length 30 mm. The exception were some joints glued with PU. The percentages of the ratio of total reaction moments and proportional moments for tenon lengths 20 mm were ranged from 74% to 77% for the standard tenon joints and from 86% to 110% for the double tenon joints. The percentages of the same ratio for tenon lengths 30 mm were higher and were ranged from 91% to 117% for the standard tenon joints and from 122% to 138% for the double tenon joints.

Table 6. Experimental Results of Displacements and the Ratios of Forces and Displacements of the Standard Mortise and Tenon Joints

Standard mortise and tenon joint											
Tenon length 20 mm						Tenon length 30 mm					
Glue	Joint No.	δ_{max} (mm)	F_{max}/δ_{max} (N/mm)	δ_p (mm)	F_p/δ_p (N/mm)	Glue	Joint No.	δ_{max} (mm)	F_{max}/δ_{max} (N/mm)	δ_p (mm)	F_p/δ_p (N/mm)
PVAc1	1	19.04	52.28	10.81	64.57	PVAc1	1	23.67	59.39	13.72	69.42
	2	17.04	76.97	11.47	76.13		2	22.46	64.08	9.42	88.31
	3	14.55	74.99	11.41	72.28		3	22.05	63.41	11.30	82.89
	Ave.	16.87	68.08	11.23	70.99		Ave.	22.73	62.29	11.48	80.21
PVAc2	1	17.60	49.16	12.57	58.17	PVAc2	1	22.16	54.07	13.47	59.15
	2	20.77	49.26	11.25	62.98		2	-	-	-	-
	3	18.29	57.87	12.31	67.87		3	21.35	55.57	8.95	84.31
	Ave.	18.89	52.09	12.04	63.01		Ave.	21.76	54.82	11.21	71.73
PU	1	19.14	66.42	12.81	68.16	PU	1	22.53	65.32	12.77	74.88
	2	14.25	70.28	8.92	79.01		2	24.17	64.68	13.38	71.46
	3	16.04	63.00	10.44	68.61		3	24.85	62.48	15.68	68.96
	Ave.	16.47	66.57	10.72	71.93		Ave.	23.85	64.16	13.94	71.77

The values of displacements at the ultimate applied load (δ_{max}), displacements at the proportional limit (δ_p) and ratios F_{max}/δ_{max} and F_p/δ_p for the standard and double tenon joints and tenon lengths 20 and 30 mm are given in Tables 6 and 7, respectively.

The percentages of the average ratio of proportional and maximal displacement of the standard tenon joints with tenon length 20 mm were approximately 66%, while this ratio percentage was from 51% to 58% for all other joints sets.

The ratios of forces at the ultimate applied load and displacement at the ultimate applied load was less than the same ratio at the proportional limit for both joint types and both tenon lengths, *i.e*., the joints stiffness was higher for the load below the proportional limit. The double mortise and tenon joints glued with PU and tenon length 30 mm had the highest average values of joints stiffness (92.3 N/mm at ultimate applied load and 118.4 N/mm at the proportional limit). The standard mortise and tenon joints glued with PVAc2 and with tenon length 20 mm had the lowest average joints stiffness at the ultimate applied load (52.1 N/mm) and at the proportional limit (63.0 N/mm). The presented results are not able to determine the effect of tenon length and glue types on the joints stiffness.

Table 7. Experimental Results of Displacements and the Ratios of Forces and Displacements of the Double Mortise and Tenon Joints

Double mortise and tenon joint											
Tenon length 20 mm						Tenon length 30 mm					
Glue	Joint No.	δ_{max} (mm)	F_{max}/δ_{max} (N/mm)	δ_p (mm)	F_p/δ_p (N/mm)	Glue	Joint No.	δ_{max} (mm)	F_{max}/δ_{max} (N/mm)	δ_p (mm)	F_p/δ_p (N/mm)
PVAc1	1	23.17	73.77	11.36	92.40	PVAc1	1	21.63	75.75	12.34	87.02
	2	18.59	79.90	9.10	100.38		2	23.82	77.35	13.10	90.77
	3	18.98	96.43	10.48	110.92		3	23.26	106.59	11.46	126.88
	Ave.	20.24	83.37	10.31	101.23		Ave.	22.91	86.56	12.30	101.56
PVAc2	1	23.65	80.44	13.27	96.93	PVAc2	1	24.32	86.28	12.66	103.91
	2	23.30	75.82	11.63	94.58		2	23.51	86.03	10.20	125.48
	3	21.43	87.72	12.28	94.13		3	24.30	68.34	18.75	65.90
	Ave.	22.79	81.33	12.39	95.22		Ave.	24.04	80.22	13.87	98.43
PU	1	20.00	81.04	11.07	99.83	PU	1	22.17	102.34	13.19	125.04
	2	14.17	80.65	7.28	95.17		2	23.48	76.95	12.38	99.36
	3	16.77	93.79	8.81	110.46		3	22.57	97.60	10.00	130.85
	Ave.	16.98	85.16	9.05	101.82		Ave.	22.74	92.29	11.86	118.42

The total reaction moments of the joints obtained from analytical calculation were used in a simplified numerical analysis of stress and strain of the loaded joints. The physical model was defined based on the experimental loading diagram of the joints, as shown in Fig. 2. Loading reaction forces (F_R) of each model of joints were calculated by the equation $F_R=M_R / d$ where M_R is analytical total reaction moment and d is the moment arm. The values of loading forces used in numerical calculations are presented in Table 8.

Table 8. Analytical Reaction Moments (Forces) and Numerical Displacement Results for Standard and Double Tenon Joints

	Standard mortise and tenon joint		Double mortise and tenon joint	
	Tenon length		Tenon length	
	20 mm	30 mm	20 mm	30 mm
M_R (Nm)	120.46	186.73	208.07	350.32
F_R (N)	587.44	910.61	1014.68	1708.38
δ_l (mm)	2.14	3.26	2.32	3.81

The numerical results of displacements of the defined point in the direction of the force F_R for standard and double tenon joints are shown in Table 8. Displacement results of loaded standard and double mortise and tenon joints are shown in Fig. 7. The maximum values of this translation displacement component occurred at the loaded end of the joint.

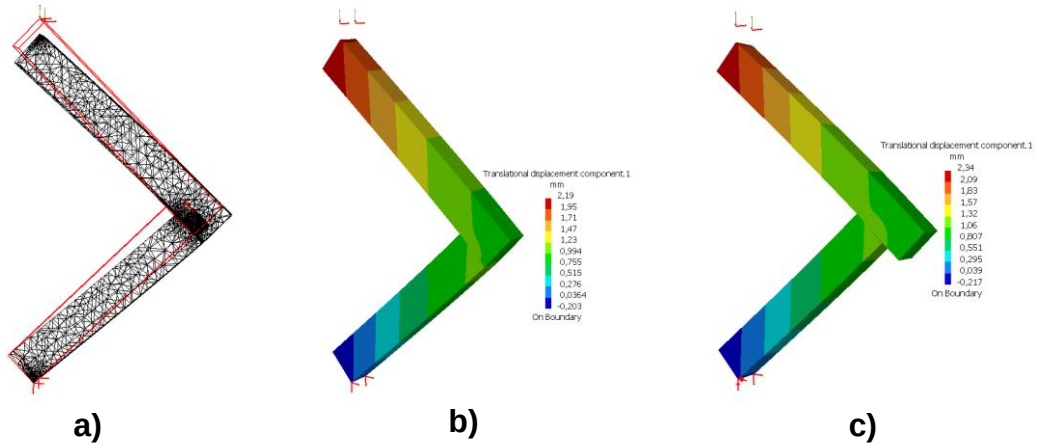

Fig. 7. Numerical result of strain analysis (tenon length 20 mm): a) deformation of the standard joint, b) and c) distribution of translational displacement component in the force direction of the standard mortise and tenon joint and double mortise and tenon joint, respectively

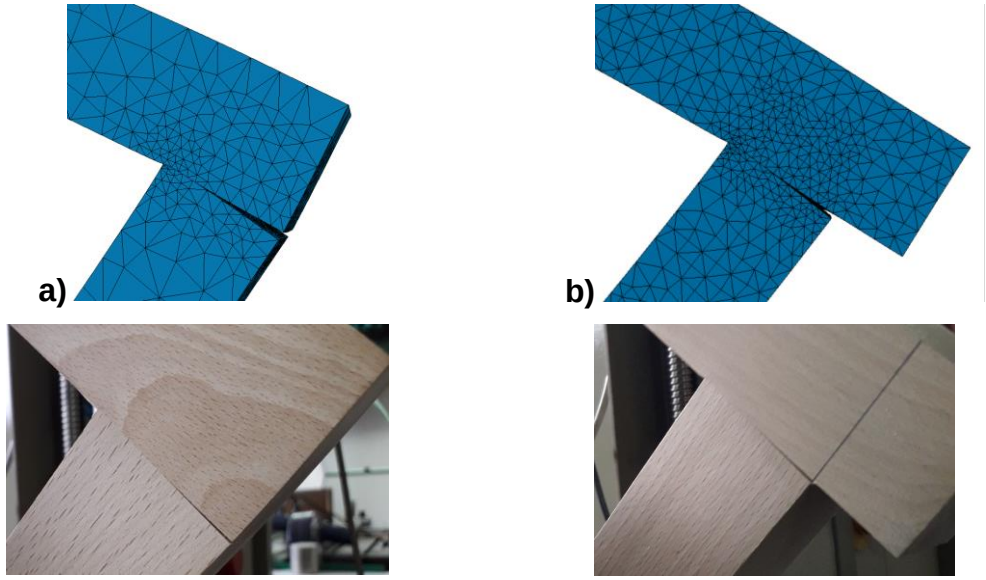

Fig. 8. Deformations obtained by numerical calculation and the test (tenon length 20 mm): a) standard mortise and tenon joint, b) double mortise and tenon joint

The joint deformations were obtained by numerical calculation and the test shows that a gap occurred among the tenon shoulder and the mortise wall in the tension zone of the joint, Fig. 8. The gap appeared due to the deformation of the mortise wall in the pressure zone of the joint *i.e.* due to the different values of the modulus of elasticity perpendicular to the fibers and parallel to the fibers.

The load-displacement graph of the standard mortise and tenon joint and double mortise and tenon joint for both tenon lengths obtained by numerical and experimental methods is shown in Fig. 9. Experimental data were obtained by analyzing only the linear elastic zone *i.e.* the initial nonlinear zone was excluded. Based on the numerical results, the percentages of the ratio of displacement for tenon lengths 20 mm and tenon length 30 mm was 66% the standard tenon joints and 61% for the double tenon joints which were approximately the same as the ratio of total reaction moment for tenon lengths of 20 mm and tenon lengths of 30 mm. As can be seen in Fig 9, increasing the tenon length from 20 mm to 30 mm for both of type joints did not increase the stiffness. This means that the joint with a tenon length 30 mm kept the achieved rigidity to a higher load. Also, the experimental results did not show a quite defined and remarkable effect of the tenon length on stiffness at the proportional limit of the standard and double mortise and tenon joints. The numerical results showed much smaller displacements of the point, *i.e.*, much higher stiffness of the joints than the displacements measured in the testing. A comparison of the numerical and experimental results indicates that the accuracy of the established models with the introduced simplifications and assumptions is not large but it was still capable to predict behavior of loaded joints in the domain of linear-elastic deformation.

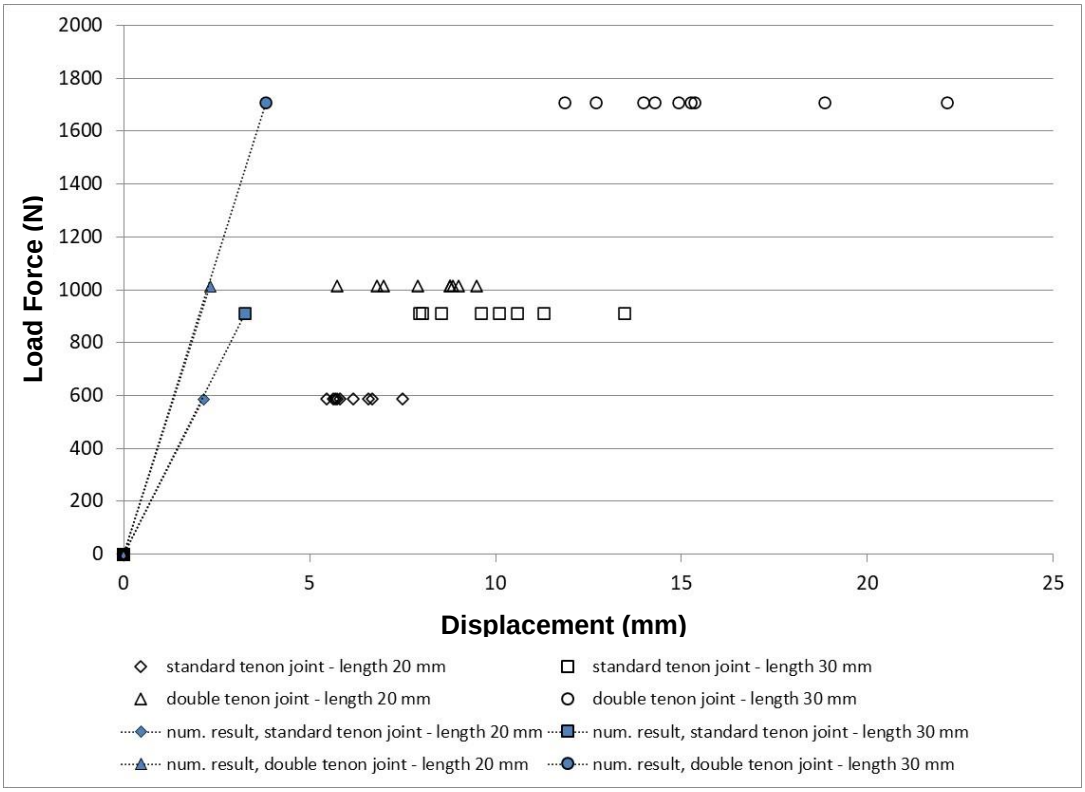

Fig. 9. Load-displacement graph of standard mortise and tenon joint and double mortise and tenon joint obtained by numerical calculation and the test (linear elastic zone only)

The distribution of effective stress (the Von Mises stress) in the standard and double mortise and tenon joints for both tenon length are shown in Figs. 10 and 11.

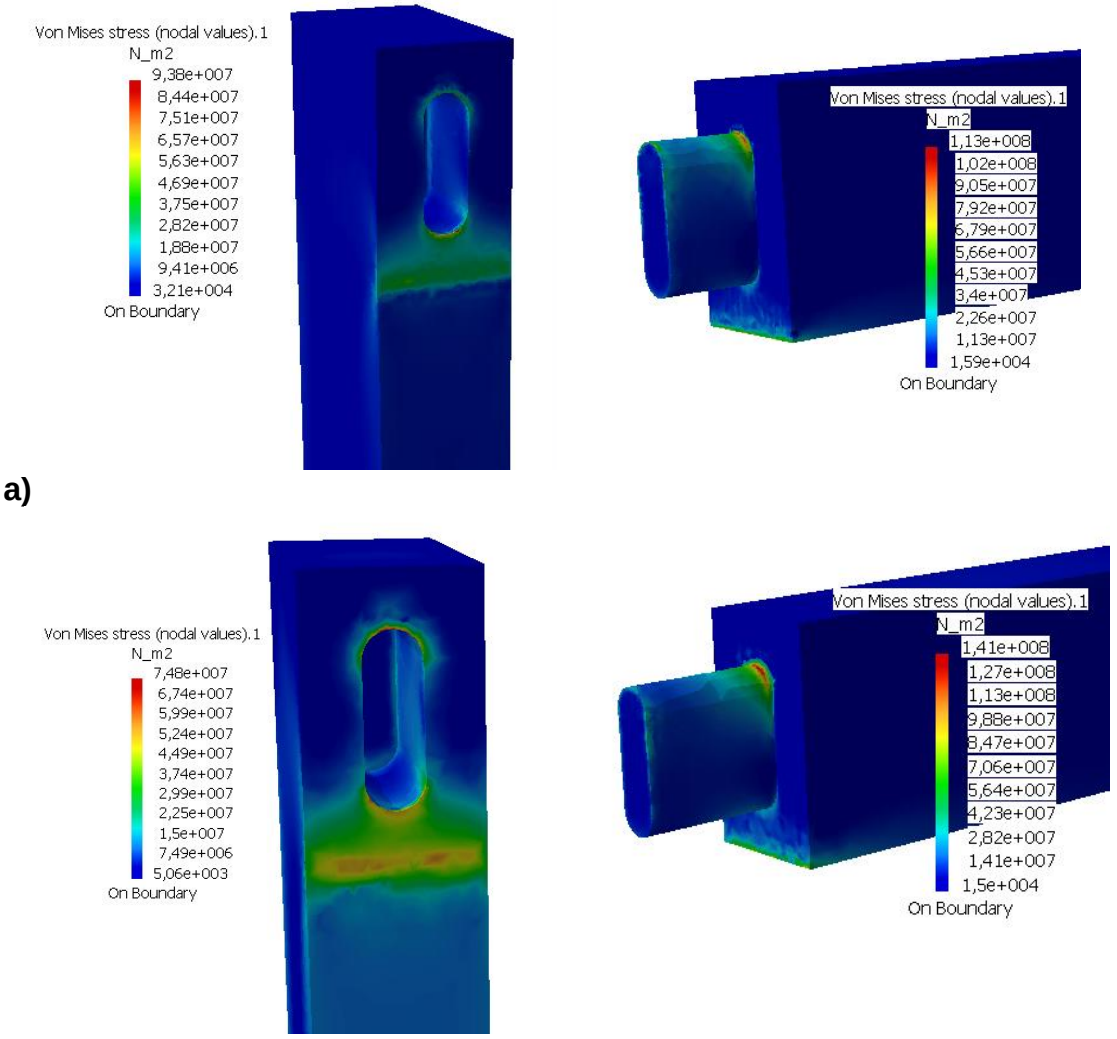

Fig. 10. Distribution of von Mises stress of standard mortise and tenon joints: a) tenon length 20 mm, b) tenon length 30 mm

The Von Mises stress is commonly used approximation that assumes that the material is isotropic and it can be a sufficiently good indicator of the stress state of a loaded construction made of orthotropic material. The maximum and increased values of von Mises stress occurred in the lower edge zone of mortise piece and in the zone of tenon upper edge cheek and in the lower zone of tenon shoulder. These zones are, along with the tenon cheeks, the places where the highest deformations and eventually fractures occurred. All other joint surfaces sustained smaller stress.

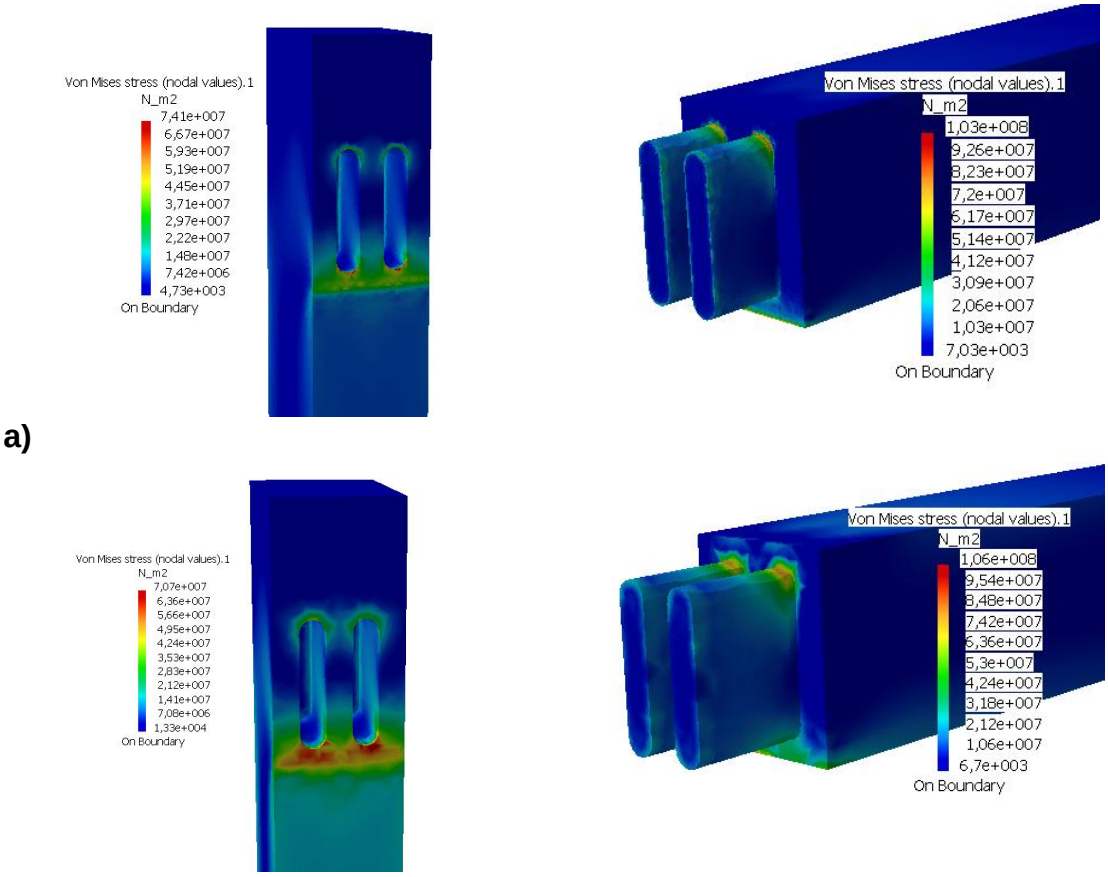

Fig. 11. Distribution of von Mises stress of double mortise and tenon joints: a) tenon length 20 mm, b) tenon length 30 mm

CONCLUSIONS

1. The tenon length has an effect on the maximal moment (moment capacity) and the proportional moment of the standard mortise and tenon joint and double mortise and tenon joint. The value of the maximal moment and the proportional moment increased as tenon length increased for both joint types and all three used glues (PVAc1, PVAc2, and PU). The joints constructed by using PU glue had a higher percentage increase than those with PVAc glue.
2. The percentage of the ratio of an average value of proportional and maximal moment of the standard tenon joints with tenon length 20 mm was above 70% for all glue type. These percentages were lower for all other set of joints, and those percentages were approximately 64%.
3. The differences among the average experimental value of joint stiffness with two different tenon lengths (20 mm and 30 mm) for both analyzed joint types and all three used glues (PVAc1, PVAc2, and PU) were not clearly observed.
4. Joint stiffness was higher for the load below the proportional limit for both joint types, both tenon lengths and glues. The double mortise and tenon joints glued with PU and with tenon length 30 mm had the highest average values of joints stiffness.

5. Analytical calculated reaction moments increased more than experimental moment values as tenon length increased for both standard and double tenon joints. The ratio of the reaction moment for tenon length 20 mm and for tenon length 30 mm was approximately under two thirds for both standard and double tenon joints. The analytical reaction moments had lower values than maximal moment (moment capacities) for all types of joints and tenon lengths. In fact, the reaction moment had generally lower values than the proportional moments for the standard mortise and tenon joints as opposed to the double mortise and tenon joints.
6. The numerical results of displacement showed much higher stiffness of the joints than the stiffness obtained by the test. Von Mises stress distribution of the loaded joints showed the characteristic zones of the maximum and increased stress values likewise those monitored in the analytical calculations.
7. Numerical and analytical results show that the presented procedures could be successfully used to achieve approximate data of mechanical properties of wood structures and joints and that are capable to estimate behavior of loaded profile adhesive joints in the linear elastic range.

REFERENCES CITED

Bardak, T., Tankut, A. N., Tankut, N., Aydemir, D., and Sozen, E. (2017). "The bending and tension strength of furniture joints bonded with polyvinyl acetate nanocomposites," *Maderas. Ciencia y Tecnología* 19(1), 51-62. DOI: 10.4067/S0718-221X2017005000005

Derikvand, M., Ebrahimi, G., and Eckelman, C. A. (2014). "Bending moment capacity of mortise and loose-tenon joints," *Wood and Fiber Science* 46(2), 1-8.

Derikvand, M., and Pangh, H. (2016). "A modified method for shear strength measurement of adhesive bonds in solid wood," *BioResources* 11(1), 354-364. DOI: 10.15376/biores.11.1.354-364

Elek, L., Kovács, Z., Csóka, L., and Agarwal, C. (2020). "Evaluation of the effect of optimal fit criteria on the compressive strength of open mortise and tenon corner joints," *European Journal of Wood and Wood Products* 78, 351-363. DOI: 10.1007/s00107-020-01509-w

Hajdarević, S., and Busuladžić, I. (2015). "Stiffness analysis of wood chair frame," *Procedia Engineering* 100, 746-755. DOI: 10.1016/j.proeng.2015.01.428.

Hajdarević, S., and Martinović, S. (2014). "Effect of tenon length on flexibility of mortise and tenon joint," *Procedia Engineering* 69, 678-685. DOI: 10.1016/j.proeng.2014.03.042.

Horman, I., Hajdarević, S., Martinović, S., and Vukas, N. (2010). "Numerical analysis of stress and strain in a wooden chair," *Drvna Industrija* 61(3), 151-158.

Hrovatin, J., Zupančič, A., Šernek, M., and Oblak, L. (2013). "The fracture moment of corner joint bonded by different glues," *Drvna Industrija* 64 (4), 335-340. DOI: 10.5552/drind.2013.1248

Hu, W., and Guan, H. (2017). "Research on withdrawal strength of mortise and tenon joint by numerical and analytic methods," *Wood Research* 62(4), 575-586.

Hu, W., Wan, H., and Guan, H. (2019a). "A finite element model of semi-rigid mortise-and-tenon joint considering glue line and friction coefficient," *Journal of Wood*

Science 65, Article number 14. DOI: 10.1186/s10086-019-1794-4

Hu, W., Wan, H., and Guan, H. (2019b). "Size effect on the elastic mechanical properties of beech and its application in finite element analysis of wood structures," *Forests* 10, 783. DOI: 10.3390/f10090783

ISO 13061-1 (2014). "Physical and mechanical properties of wood-Test methods for small clear wood specimens – Part 1: Determination of moisture content for physical and mechanical test," International Organization for Standardization, Geneva, Switzerland.

Kasal, A., Eckelman, C. A., Haviarova, E., Erdil, Y. Z., and Yalcin I. (2015). "Bending moment capacities of L-shaped mortise and tenon joints under compression and tension loadings," *BioResources* 10(4), 7009-7020. DOI: 10.15376/biores.10.4.7009-7020.

Kasal, A., Smardzewski, J., Kuşkun, T., and Erdil, Y. Z. (2016). "Numerical analyses of various sizes of mortise and tenon furniture joints," *BioResources* 11(3), 6836-6853. DOI: 10.15376/biores.11.3.6836-6853

Likos, E., Haviarova, E., Eckelman, C. A., Erdil, Y. Z., and Ozcifci, A. (2012). "Effect of tenon geometry, grain orientation, and shoulder on bending moment capacity and moment rotation characteristics of mortise and tenon joints," *Wood and Fiber Science* 44(4), 462-469.

Máchová, E., Langová, N., Réh, R., Joščák, P., Krišťák, L., Holouš, Z., Igaz, R., and Hitka, M. (2019). "Effect of moisture content on the load carrying capacity and stiffness of corner wood-based and plastic joints, " *BioResources* 14(4), 8640-8655. DOI: 10.15376/biores.14.4.8640-8655

Podlena, M., and Borůvka, V. (2016). "Stiffness coefficients of mortise and tenon joints used on wooden window profiles," *BioResources* 11(2), 4677-4687. DOI: 10.15376/biores.11.2.4677-4687.

Podlena, M., Böhm, M., Múčka, M., and Bomba, J. (2017). "Determination of the bending moment of a dowel and tenon joint on window profile IV 92 of a wooden window," *BioResources* 12(2), 4202-4213. DOI: 10.15376/biores.12.2.4202-4213.

Skarvelis, M., and Mantanis, G. I. (2013). "Physical and mechanical properties of beech wood harvested in the Greek public forests," *Wood Research* 58(1), 123-130.

Smardzewski, J. (2008). "Effect of wood species and glue type on contact stresses in a mortise and tenon joint," *Journal of Mechanical Engineering Science* 222(12), 2293-2299. DOI: 10.1243/09544062JMES1084.

Vassiliou, V., Barboutis, I., and Kamperidou, V. (2016). "Strength of corner and middle joints of upholstered furniture frames constructed with black locust and beech wood," *Wood Research* 61(3), 495-504.

Wilczyński, A., and Warmbier, K. (2003). "Effect of joint dimensions on strength and stiffness of tenon joints," *Folia Forestalia Plonica, Seria B, Zeszyt* 34, 53-66.

Záborský, V., Borůvka, V., Kašičková, V., and Ruman, D. (2017). "Effect of wood species, adhesive type, and annual ring directions on the stiffness of rail to leg mortise and tenon furniture joints," *BioResources* 12(4), 7016-7031. DOI: 10.15376/biores.12.4.7016-7031

Article submitted: May 1, 2020; Peer-review completed: June 29, 2020; Revised version received and accepted: July 24, 2020; Published: September 14, 2020.
DOI: 10.15376/biores.15.4.8249-8267